



# Experimental investigation of firebrand accumulation zones in front of obstacles



Sayaka Suzuki<sup>a,\*</sup>, Samuel L. Manzello<sup>b</sup>

<sup>a</sup> Large Fire Laboratory, National Research Institute of Fire and Disaster (NRI), Chofu, Tokyo 182-0012, Japan

<sup>b</sup> Fire Research Division, National Institute of Standards and Technology (NIST), Gaithersburg, MD 20899-8662, USA

## ARTICLE INFO

### Keywords:

Large outdoor fire  
Wildland-urban interface (WUI) fire  
Urban fires  
Firebrand accumulation  
Wind-driven firebrands

## ABSTRACT

It is well accepted that as structures are exposed to wind, stagnation planes are produced around structures. Past work by the authors demonstrated for the first-time that wind-driven firebrand showers may accumulate in these stagnation planes. While those experiments demonstrated this important phenomenon, due to the limited duration of firebrand showers of the original NIST Batch-Feed Firebrand Generator, it was not possible to perform a more systematic study. To this end, a series of detailed experiments were performed using the recently developed NIST Continuous-Feed Firebrand Generator capable of firebrand showers of unlimited duration. Full-scale walls of varying size were placed downstream of the device and the wind speed was varied in increments up to 10 m/s. The experiments were conducted in the Building Research Institute's Fire Research Wind Tunnel Facility (FRWTF). For a given wall size exposed to specific firebrand size/mass distribution, it was observed that wind speed influences not only the spatial location and extent of the accumulated firebrands in the stagnation plane in front of the wall, but also the nature of the smoldering combustion intensity of the accumulated firebrands. The experiments demonstrated that higher wind speeds (10 m/s) did not promote accumulation of firebrands in stagnation planes in front of walls. The data may be used to provide guidance to appropriate separation distances that combustibles should be placed near structures and is also of great use to develop and validate numerical models of firebrand accumulation.

## 1. Introduction

Wildfires that spread into communities, referred to as Wildland-Urban Interface (WUI) fires, have destroyed communities throughout the world. The Witch Fire of 2007 in Southern California forced 300,000 people to evacuate, destroyed over one thousand structures, and resulted in \$1B (USD) paid by insurers [1]. In Europe, the 2007 fires in Greece destroyed several hundred structures, and resulted in the deaths of more than 70 people. In Australia, the 2009 fires in Victoria caused the death of 173 people and destroyed more than one thousand structures [2]. WUI fires have also ravaged Chile recently [3].

Japan does not have a specific problem of fires spreading from the wildlands to communities, such as the WUI fire problem in the USA and other countries [4]. Rather, Japan experiences many earthquakes. After large earthquakes, many fires may simultaneously occur that can easily overwhelm firefighting resources. Since most Japanese cities are densely populated, severe fire spread occurs within these urban areas [4].

Fire safety science research has spent a great deal of effort to

understand fire dynamics within buildings. Research into large outdoor fires, such as WUI and urban fires, and how to potentially mitigate the loss of structures in such fires, is far behind other areas of fire safety science research. This is due to the fact that large outdoor fire spread is incredibly complex, involving the interaction of topography, weather, vegetation, and structures [1].

An interesting similarity, that is a major factor in both WUI and urban fire spread, is firebrand production. When vegetation and structures burn in these fires, pieces of burning material, known as firebrands, are generated, become lofted, and are carried by the wind. This results in showers of wind-driven firebrands.

While firebrand showers are responsible for a majority of structure ignitions in WUI fires (see any number of post-fire investigation reports over the past 60 years; for example [5–9]), no science-based standard laboratory methods exist to evaluate individual building component's resistance to ignition from wind-driven firebrand showers. Without standard laboratory test methods, it is impossible to evaluate and compare the performance of building component's ability to resist

\* Corresponding author.

E-mail address: [sayakas@fri.go.jp](mailto:sayakas@fri.go.jp) (S. Suzuki).

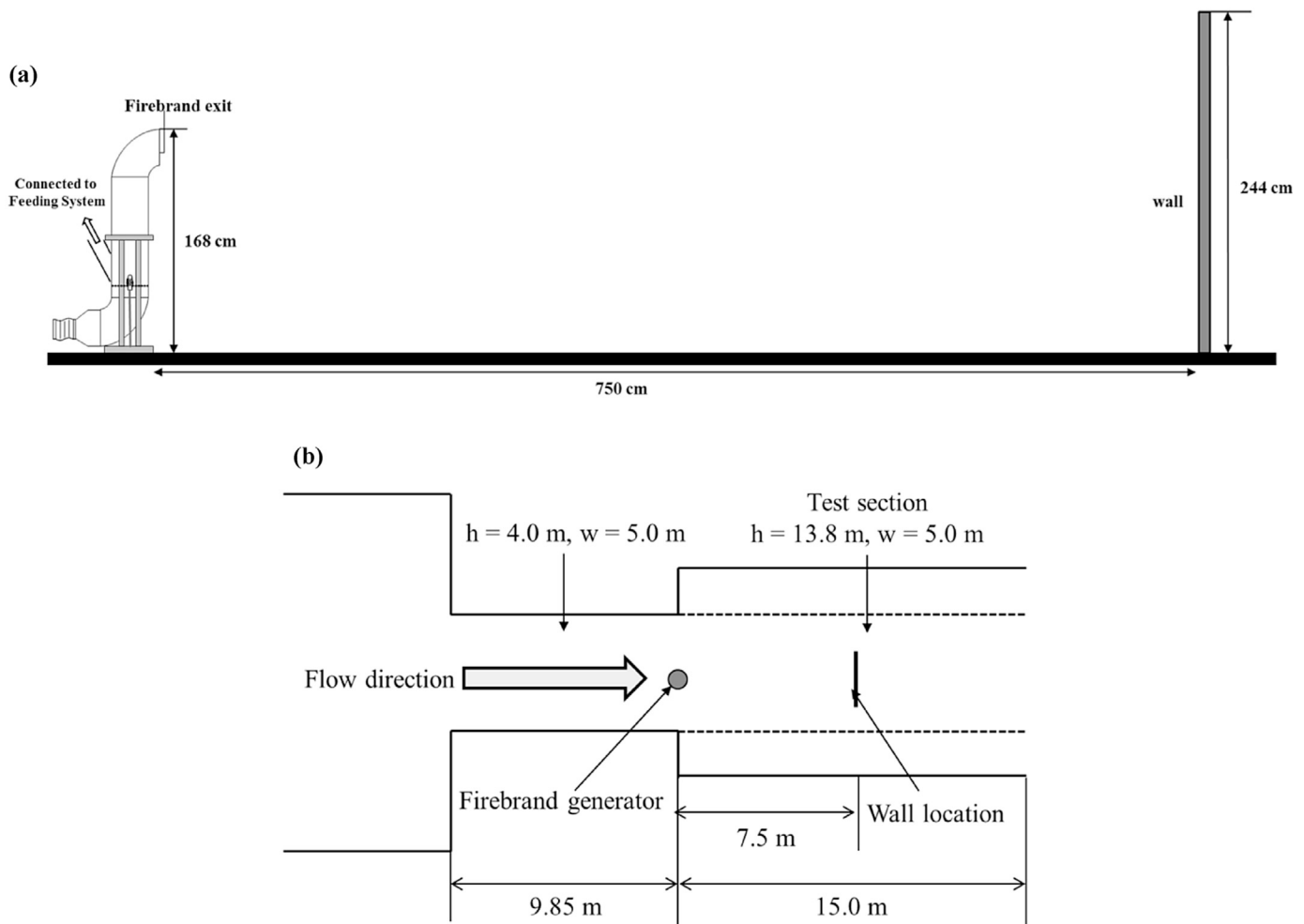


Fig. 1. (a) Schematic of locations of the continuous-feed firebrand generator and a wall (side view). (b) Schematic of locations of the continuous-feed firebrand generator and a wall (Top view).

firebrand ignition. It cannot be overstated that current understanding of building component type to WUI exposure is still mainly predicated on *anecdotal* evidence. As a result, the limited WUI fire and building codes and standards in practice lack scientific rigor and, when implemented, it is not clear if these provide any benefit to structures in the path of hazardous WUI fires [10]. In Japan, several city fire spread models were developed for estimation of damage. These models were based on the real city fires damages and empirical formula under limited situations. There is a lack of scientific and reliable data.

As structures are exposed to wind, stagnation planes are produced around structures. In a prior scoping study, the authors demonstrated that firebrands may accumulate in these stagnation planes [11]. This paper describes a more in depth study of this phenomenon. Specifically, new insights have been made possible by an improved experimental design to generate continuous wind-driven firebrand showers. While some of these results have been presented at a recent conference, this paper describes these findings for the archival literature [12].

## 2. Experimental description

Experiments were performed by using the full-scale Continuous-Feed Firebrand Generator. This version of the device is modified from the batch-feed version of the NIST Dragon, and consisted of two parts: the main body and continuous feeding component. A summary of the NIST Dragon technology has been published elsewhere so only a brief description is provided here [13]. The feeding part was connected to the

main body (Dragon) and was equipped with two gates to prevent fire spread (described in more detail below). The feeding system consisted of a pneumatic cylinder coupled to a cylindrical container where wood pieces were stored. The pneumatic cylinder was contained inside a metal sleeve, where the sliding rod of the pneumatic cylinder was connected to a plate that allowed the volume of wood contained within the sleeve to be varied. This volume was set precisely to allow a specific mass of firebrands to fall into this volume. When the air pressure was applied, the sliding rod of the pneumatic cylinder moved forward, forcing the wood pieces that had fallen by gravity within the volume of the metal sleeve to the first gate, where they were then dropped into second gate that led to the Dragon where they were ignited.

The full-scale wall with varied size was placed downstream of the device, perpendicular to the wind, and the wind speed was varied in increments of 2 m/s up to 10 m/s. Specifically, two walls with dimensions of 1.32 m (H) by 2.44 m (W), and 2.44 m (H) by 2.44 m (W) were used. Different dimensions were intentionally selected to determine the influence of the obstacle profile on potential firebrand accumulation zones. These were located at a distance of 7.5 m from the Continuous-Feed Firebrand Generator to visualize the transport process. The experiments were conducted in the Building Research Institute's Fire Research Wind Tunnel Facility (FRWTF). The FRWTF has a cross section of 4.0 m (H) by 5.0 m (W). The wind field is generated by a 4.0 m (diameter) axial fan (up to 10 m/s;  $\pm 10\%$ ). To determine if accumulated firebrands represented an ignition danger, the floor of the FRWTF was lined with gypsum board.

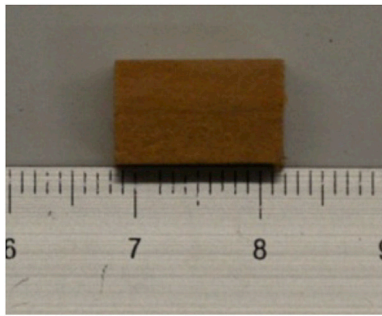


Fig. 2. Image of a Douglas-fir wood piece.

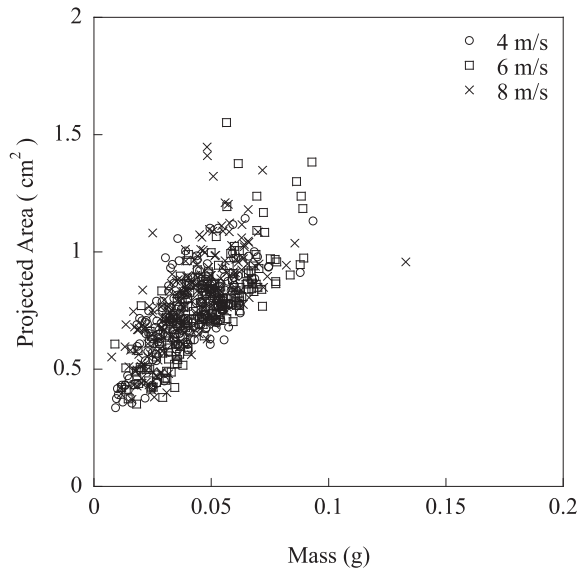


Fig. 3. Firebrand projected area vs mass for various wind speeds.

A typical experiment was conducted in the following manner. The wall assembly was installed at 7.5 m downstream of the firebrand generator, perpendicular to the wind (see Fig. 1(a) and (b)). The wind tunnel speed was set to the desired level. Wood pieces were first loaded into the cylinder storage container and the air compressor needed to provide compressed air for the pneumatic cylinder and gate system was switched on (air compressor pressure was set to 0.7 MPa). The blower was set at 3.0 m/s (for glowing firebrands) and two propane burners were ignited and inserted into the side of the device. The propane burners were operated continuously during the experiment. The pneumatic piston was then activated and the sliding rod was positioned to allow wood pieces to enter the volume in the metal sleeve. The sliding rod was moved to push the wood pieces (200g) to the first gate. The gate first was opened, closed, and the second gate was then opened, and the wood fell into the Dragon.

A very important characteristic of the NIST Dragon is that the firebrand size and mass produced using the device can be tailored to those measured from full-scale tree burns [14,15], and actual WUI fires [16]. In collaboration with the California Department of Forestry and Fire Protection (CALFIRE), NIST quantified firebrand distributions from a real WUI fire (2007 Angora Fire) [16]. Specifically, digital image analyses of burn patterns from materials exposed to the Angora Fire were conducted to determine firebrand size distributions. The firebrand size distributions reported were compared to firebrand size distributions from experimental firebrand generation using the NIST Dragon, as well as historical firebrand field studies. The most salient result reported in Ref. [16] was the documentation of the consistently small size of firebrands ( $<1.0 \text{ cm}^2$ ). The Texas Forest Service has used this methodology to collect firebrand size distributions from the recent Texas Bastrop Complex fires in 2011, as well, and reported similar findings to the 2007 Angora fire; significant numbers of very small firebrands were produced [17]. It cannot be stressed enough that more data is needed from actual WUI and urban fires.

For all tests, Douglas-fir wood pieces, shown in Fig. 2, machined to dimensions of 7.9 mm (H) by 7.9 mm (W) by 12.7 mm (L) were used to produce firebrands. Firebrands generated from these sized wood pieces have been shown to be commensurate to firebrand sizes measured from full-scale burning trees as well firebrand size distributions obtained from actual WUI fires [11,16,17]. The mass flux of generated firebrands may

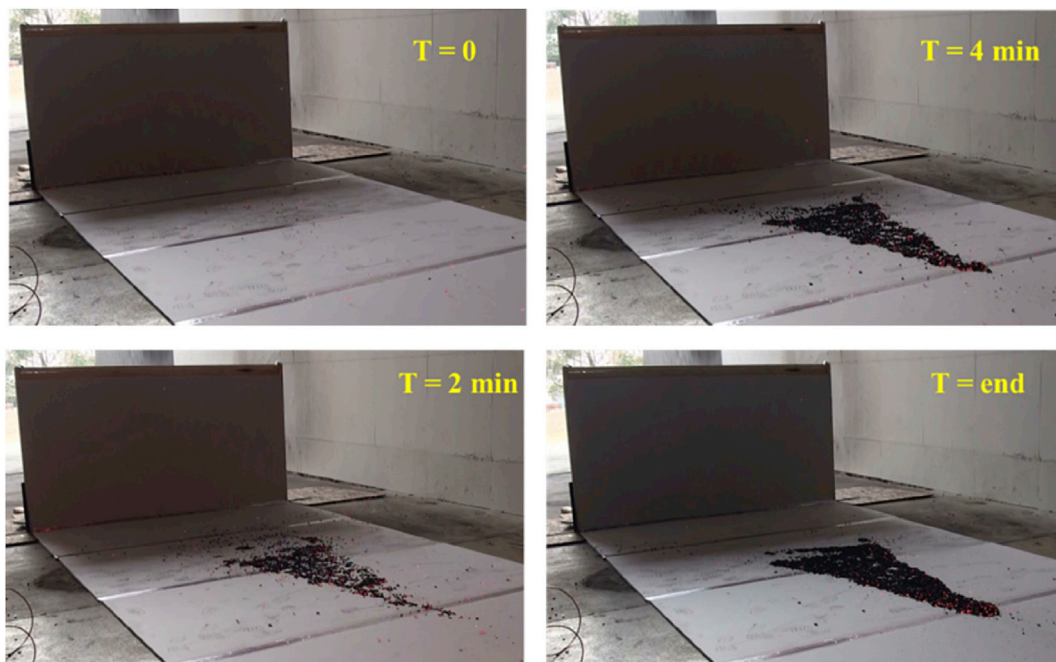


Fig. 4. Images of firebrand accumulation as time with 1.32 m (H) by 2.44 m (W) obstacle under 6 m/s wind.



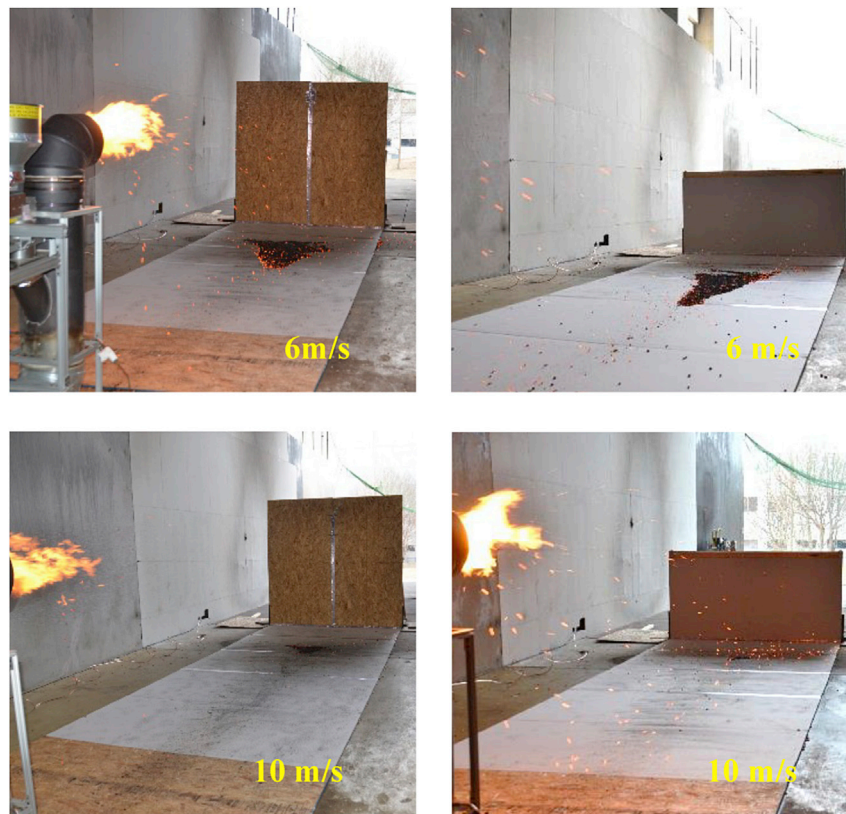


Fig. 5. Firebrand accumulations. Left: 2.44 m (H) by 2.44 m (W) obstacle and Right: 1.32 m (H) by 2.44 m (W) obstacle.

be adjusted by varying the feeding rate of wood pieces into the device; a wood feeding rate of 800 g/min was used in these experiments, which resulted in a mass flux of firebrands of  $17.1 \text{ g/m}^2\text{s}$ . Details regarding the methodology to determine the mass flux are provided elsewhere [13].

The firebrand size and mass distribution was determined as a function of wind speed. Separate experiments were conducted by placing an array of pans downstream of the firebrand generator. The presence of the water quenches the combustion process. The firebrands are subsequently removed from the water pans, dried and image analysis is conducted to determine the projected area of the generated firebrands as a function of wind speed (described in detail below).

Fig. 3 displays the influence of wind speed on the projected area of the generated firebrands. Image analysis software was used to determine the projected area of a firebrand by converting the pixel area using an appropriate scale factor [18]. It was assumed that deposited firebrands would rest flat on the ground and the projected areas with the maximum dimension and the second maximum dimension of three dimensions were measured (for cylindrical and flat shaped firebrands respectively)

[18]. Images of well-defined shapes (e.g. circular objects) were used to determine the ability of the image analysis method to calculate the projected area [18]. Based on repeat measurements of different areas, the standard uncertainty in determining the projected area was  $\pm 10\%$ . The mass of each firebrand was measured by a precision balance with 0.001 g resolution. Repeat measurements of known calibration masses were measured by the balance which was used for the firebrand mass analysis. The standard uncertainty in the firebrand mass was calculated to be between 1 (for the largest firebrand) and 10 (for the smallest firebrand) %.

As can be seen, the distribution of projected area as a function of firebrand mass did not vary significantly as the wind speed was increased. As a result, observations in this study are believed to be simply due to changes of the flow distribution around the obstacles as the wind speed was increased.

### 3. Results and discussion

In all experiments, the same amount of wood pieces was fed into Dragon so that all the walls were attacked by firebrand showers for the same duration. In total, 10 min of feeding, which corresponds to 8 kg of wood pieces, was provided. Fig. 4 displays images of time dependent firebrand accumulations. Within a few minutes firebrands were accumulated in one zone. As time goes, it was observed the firebrands arrived on the accumulated area, thus more covered in the area, yet the size of the accumulated area did not change. Some firebrands landed in front of wall, some flew out and landed in the back of wall, and others hit the wall and landed and moved downwind or upwind. Different behaviors of firebrands under different wind speed were observed.

Fig. 5 (Left) displays images of the experiments conducted with 2.44 m (H) by 2.44 m (W) obstacle placed downstream of firebrand showers (6 m/s and 10 m/s are shown). At a wind speed of 4 m/s (not shown), the firebrands were unable to accumulate into compact zones,



Fig. 6. Accumulated firebrands have been swept off after the completion of the experiments. Multiple ignition points of the gypsum board paper are observed.

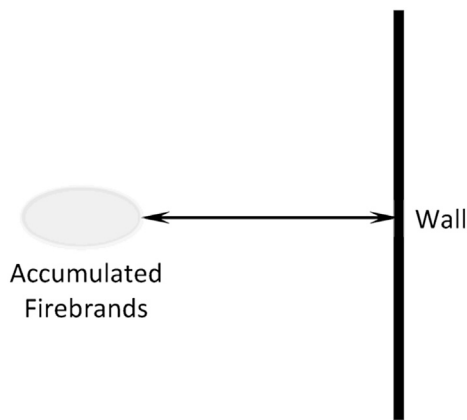


Fig. 7. Separation distance from the wall (obstacle) to the area of accumulated firebrands.

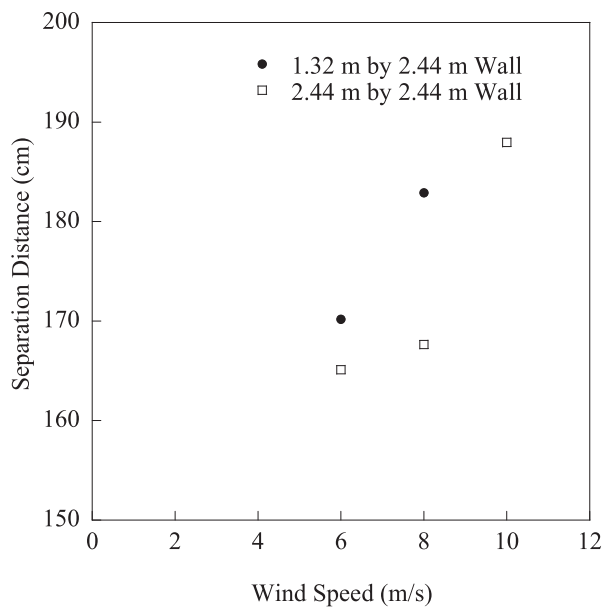


Fig. 8. Measured separation distance from the wall to the area of accumulated firebrands.

and as a result, were unable to collectively use the heat generated from individual firebrand combustion to ignite the paper of the gypsum board. At 6 m/s, the most significant accumulation was observed and the accumulated heat provided sufficient heat feedback to ignite the paper of the gypsum board. Little accumulation was observed at the highest wind speed used (10 m/s).

Fig. 5 (Right) displays images of the experiments conducted with 1.32 m (H) by 2.44 m (W) obstacle placed downstream of firebrand showers (6 m/s and 10 m/s are shown). Similar to the experiments with the 2.44 m by 2.44 m wall, at a wind speed of 4 m/s (not shown), the firebrands were unable to accumulate into compact zones, and as a result, were unable to collectively use the heat generated from individual firebrand combustion to ignite the paper of the gypsum board. At 6 m/s, the most significant accumulation was observed and the accumulated firebrands provided sufficient heat feedback to ignite the paper of the gypsum board (see Fig. 6). No accumulation was observed at the highest wind speed used (10 m/s). For both obstacles, it is believed that at the highest wind speed of 10 m/s, little or no firebrand accumulation was observed due to the enhanced flow recirculation present afforded by the higher wind speeds. Yet, as discussed below, additional firebrand distributions must be compared to the present data.

The multiple smoldering ignitions on the paper of the gypsum board were observed in experiments under 6 m/s and 8 m/s wind speed. The

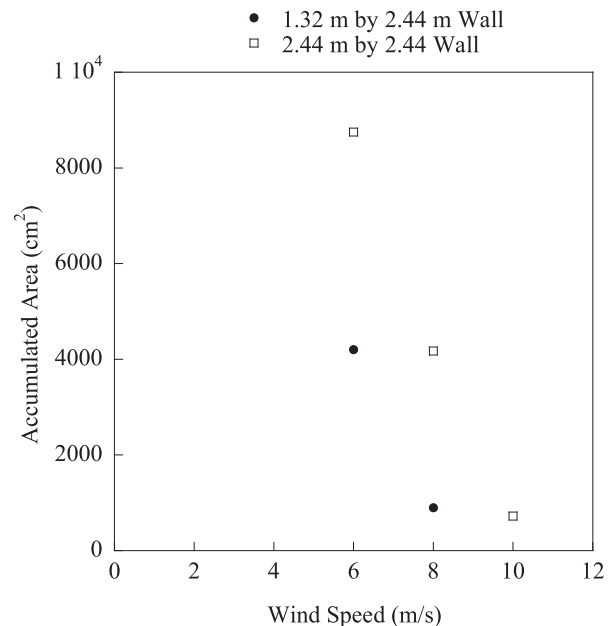


Fig. 9. Measured area of accumulated firebrands. It was not possible to determine the accumulated firebrand area for the 1.32 m by 2.44 m wall at 10 m/s since it was not possible for firebrands to accumulate anymore at the highest wind speed considered.

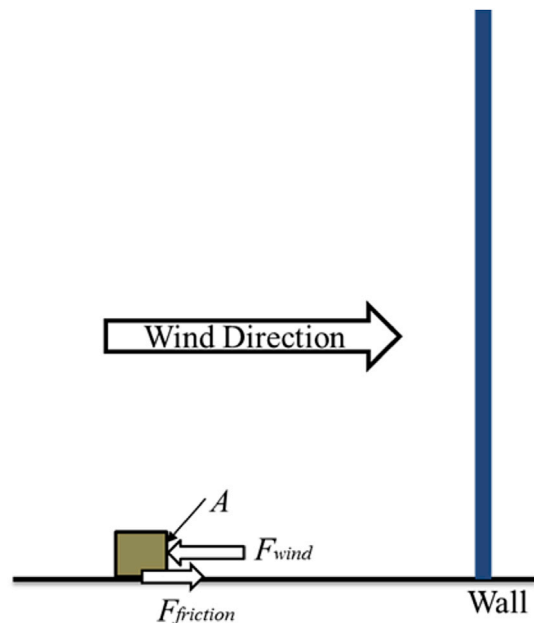


Fig. 10. Schematics of force balance on a firebrand.

most severe ignitions were observed in the experiments with 6 m/s wind speed (see Fig. 6) rather than higher wind speeds. The smoldering ignitions were observed to be affected largely by wind speed, which also affected the accumulation patterns.

The separation distance from the wall to the area of accumulated firebrands was measured as a function of wind speed. Fig. 7 displays a schematic of demonstrating how this distance was measured and Fig. 8 is a graph of these measurements. For the 1.32 m by 2.44 m wall, no firebrand accumulation was observed at 10 m/s, and as a result, it was not possible to measure the separation distance. For both wall geometries considered, the area of accumulated firebrands was observed to move further away from the wall as the wind speed was increased.

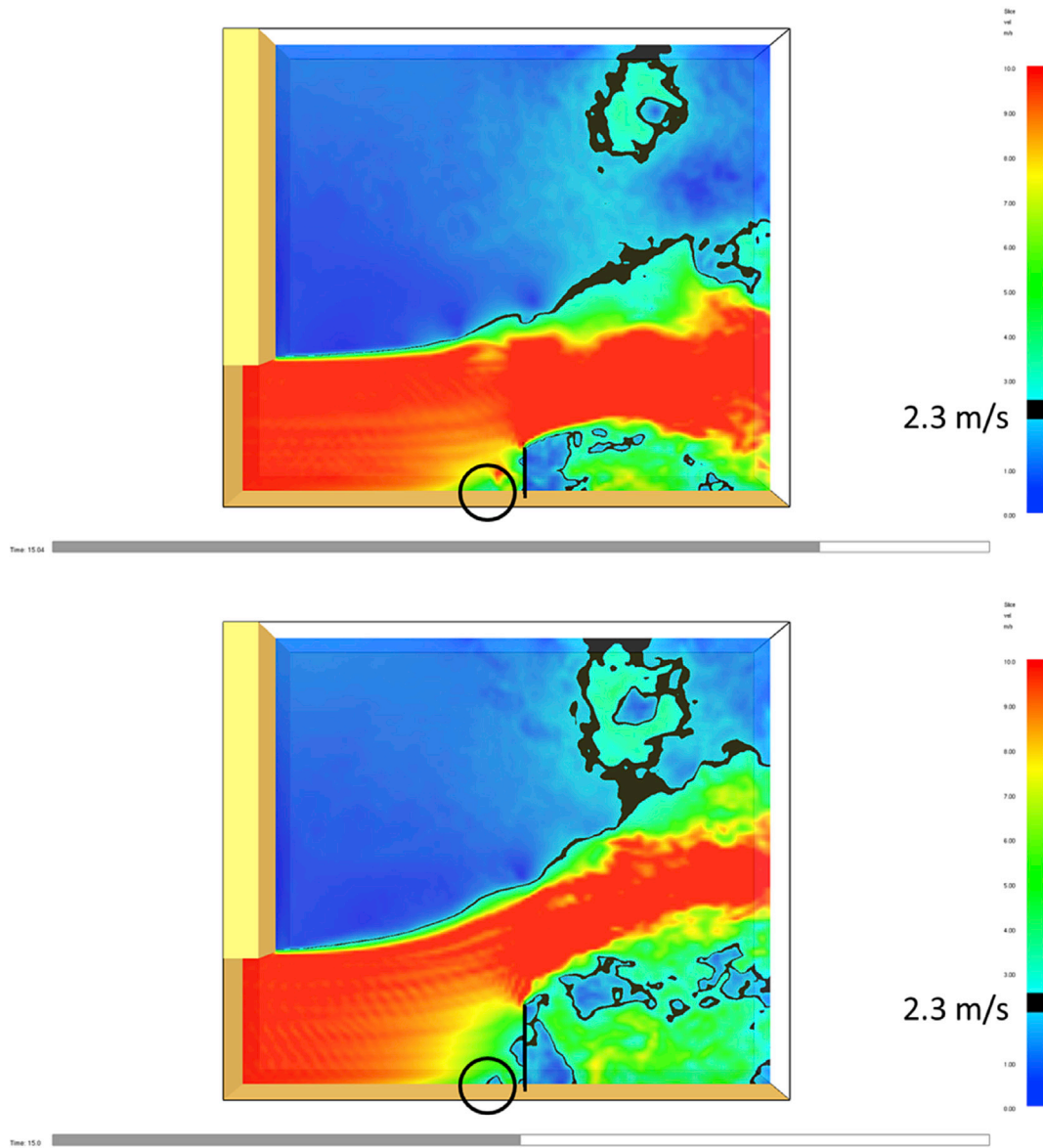


Fig. 11. FDS simulation under 10 m/s wind; with 1.32 m wall (above) and 2.44 m (below). Black line indicates wind speed of 2.3 m/s. There are no zones under 2.3 m/s wind speed in front of 1.32 m wall (above) while there are zones under 2.3 m/s wind speed in front of 2.44 m wall (below).

Fig. 9 displays the measured area of the accumulated firebrands as a function of wind speed. As the wind speed was increased, the area of accumulated firebrands was reduced significantly. These areas were also determined using image processing software. Based on repeat measurements of different areas, the standard uncertainty in determining the projected area was  $\pm 5\%$ . It is also important to mention that each wall was exposed to firebrand showers for the same duration.

While many factors have to be considered in order to understand firebrand accumulation in front of the obstacles, a very basic, first-step analysis was conducted to try to understand the observed results. In order for firebrands to accumulate, the force by wind on a firebrand ( $F_{wind}$ ) should be balanced with the friction force between the firebrand and the floor (gypsum board) ( $F_{friction}$ ) (see Fig. 10).

$$F_{friction} = F_{wind}$$

Here,

$$F_{friction} = \mu m_{firebrand} g$$

$$F_{wind} = \frac{1}{2} \rho_{air} v^2 \times A$$

Therefore,  $\mu$  is the friction coefficient between a gypsum board and smoldering firebrands,  $m_{firebrand}$  is the average mass of a firebrand,  $\rho_{air}$  is the density of the air,  $g$  is gravitation acceleration,  $v$  is wind speed on a firebrand and  $A$  is the average projected area of firebrand.

$$\mu m_{firebrand} g = \frac{1}{2} \rho_{air} v^2 \times A$$

There are no studies on friction coefficient between a gypsum board and smoldering firebrands (or any burning wood) so we assume  $\mu = 0.5$  based on the friction coefficient data between woods [19]. Also, we measured  $A = 0.78 \text{ cm}^2$  and  $m_{firebrand} = 0.05 \text{ g}$  as the average projected area and average mass of firebrands, respectively. Eventually  $v$  is calculated to be around 2.3 m/s. This means that the flow in front of obstacles allows firebrands to stay in the same place if the flow around firebrands is under 2.3 m/s.

Wind profiles without firebrands around the obstacle were simulated by using Fire Dynamics Simulator (FDS) [20]. FDS is a large eddy



simulation (LES) code for low-speed flows, with an emphasis on smoke and heat transport from fires and is also used to simulate flow without fires [31]. BRI' FRWTF was simulated by FDS with the grid size of 10 cm (Fig. 1(b)). As discussed earlier, experiments under 10 m/s wind, with 1.32 m wall and 2.44 m wall showed different behaviors of firebrand accumulation. Fig. 11 above shows there are no flow zones below 2.3 m/s with the simulation with 1.32 m wall and thus firebrands could not stay at all around the obstacles due to the flow in the simulation with 1.32 m wall. On the other hand, with 2.44 m wall, the flow under 2.3 m/s, still stably exists and thus firebrands are still able to accumulate in front of obstacles. This result matches with our experimental findings.

#### 4. Implications for firebrand accumulation modeling

By far, the study of firebrand transport has been the most studied area of firebrand research. The interested reader is referred to numerous studies on this topic [21–29]. Yet, these models are focused on understanding the spotting distance, or namely, how far firebrands may fly. It has not been possible to develop models to predict firebrand accumulation zones as there is no experimental validation data to do this. It is believed that the data presented here is of great use to validate numerical models of firebrand accumulation around structures. Such models would allow the investigation of firebrand accumulation zones over a broad parameter space (higher wind speeds, various structure facades). Through the development of such models, it may be possible to design buildings within communities in such a manner to reduce firebrand accumulation zones. Prior data collected by the authors using the firebrand generator have been used to develop and *validate* numerical models of firebrand transport [30]. This new data presented here should be of even greater use to develop models of firebrand accumulation zones around structures. Additional experiments are underway using various firebrand size and mass distributions and efforts are also in progress to use a reduced scale firebrand generator to determine if similar results are observed for much smaller sized obstacles [31].

#### 5. Summary

Research into WUI fires, and how to potentially mitigate the loss of structures in such fires, is far behind other areas of fire safety science research. Since the best way forward to address the WUI problem is the hardening of structures [32], the technical basis for improved test standards and fire and building codes is being developed.

As structures are exposed to wind, stagnation planes are produced around structures. In a prior scoping study, the authors demonstrated that firebrands may accumulate in these stagnation planes. This paper described a more in depth study of this phenomenon.

It was observed that wind speed influences not only the spatial location and extent of the accumulated firebrands in the stagnation plane in front of the obstacle, but also the nature of the smoldering combustion intensity of the accumulated firebrands. Future experiments will consider varying firebrand mass/size distributions as well as obstacles of varying aspect ratio. Experiments under wind speeds greater than 10 m/s would also be desirable.

#### Acknowledgements

The authors would like to acknowledge the many contributions from Mr. Marco Fernandez, Mr. Edward Hnetkovsky, Mr. John Shields, Mr. Laurean DeLauter, Mr. Tony Chakalis, and Mrs. Doris Rinehart, all of the Engineering Laboratory (EL) at NIST. Dr. Matthew Bundy, NIST National Fire Research Laboratory (NFRL) Director, is acknowledged for making NFRL technicians available to support this work by preparing all

materials for shipping to Japan. Dr. Ichiro Hagiwara of BRI (Japan) is appreciated for allowing us to use the Fire Research Wind Tunnel Facility to conduct the experiments outlined in this paper.

#### References

- [1] S.L. Manzello, Special issue of wildland-urban Interface (WUI) fires, *Fire Technol.* 50 (2014) 7–143.
- [2] 2009 Victorian Bushfires Royal Commission, July 2010.
- [3] P. Reszka, A. Fuentes, The great valparaiso fire and fire safety management in Chile, *Fire Technol.* 51 (2015) 753–758.
- [4] S.L. Manzello, et al., Workshop for fire structure interaction and urban and wildland-urban Interface (WUI) fires – operation tomodachi fire research, *Fire Saf. J.* 59 (2013) 122–131.
- [5] G.J. Barrow, A survey of houses affected in the beaumaris fire, January 14, 1944, *J. Coun. Sci. Industrial Res.* [now CSIRO] 18 (1945) 27–37.
- [6] R. Abt, D. Kelly, M. Kuypers, The Florida palm coast fire: an analysis of fire incidence and residence characteristics, *Fire Technol.* 23 (1987) 186–197.
- [7] E.I.D. Foote, Structure Survival on the 1990 Santa Barbara “Paint” Fire: a Retrospective Study of Urban-wildland Interface Fire Hazard Mitigation Factors, MS thesis, University of California at Berkeley, 1994, p. 129.
- [8] D.A. Gordon, Structure Survival in the Urban/Wildland Interface: a Logistic Regression Analysis of the Oakland/Berkeley Tunnel Fire, MS thesis, University of California at Berkeley, 2000, p. 447.
- [9] A. Maranghides, W.E. Mell, A case study of a community affected by the witch and guejito fires, *Fire Technol.* 47 (2011) 379–420.
- [10] S.L. Manzello, S.L. Quarles, Special Section on Structure Ignition in Wildland-Urban Interface (WUI) Fires, *Fire Technol.* 53 (2017) 425–427.
- [11] S.L. Manzello, S.H. Park, J.R. Shields, S. Suzuki, Y. Hayashi, Determining structure vulnerabilities to firebrand showers in wildland-urban Interface (WUI) fires, *Fire Saf. J.* 46 (2011) 568–578.
- [12] S.L. Manzello, S. Suzuki, Firebrand Accumulation Zones in Front of Structures in Wildland Urban Interface (WUI) Fires, *Fire and Materials Conference*, San Francisco, CA, 2015.
- [13] S.L. Manzello, Enabling the investigation of structure vulnerabilities to wind-driven firebrand showers, *Fire Saf. Sci.* 11 (2014) 83–96.
- [14] S.L. Manzello, A. Maranghides, W.E. Mell, Firebrand generation from BurningVegetation, *Int'l J. Wildland Fire* 16 (2007) 458–462.
- [15] S.L. Manzello, et al., Mass and size distribution of firebrands generated from burning Korean pine (*pinus koraiensis*) trees, *Fire Mater.* 33 (2009) 21–31.
- [16] S.L. Manzello, E.I.D. Foote, Characterizing firebrand exposure during wildland-urban Interface fires: results of the 2007 Angora fire, *Fire Technol.* 50 (2014) 105–124.
- [17] S. Rissel, K. Ridenour, Ember production during the Bastrop complex fire, *Fire Manag. Today* 72 (2013) 7–13.
- [18] S. Suzuki, S.L. Manzello, M. Lage, G. Laing, Firebrand generation data obtained from a full scale structure burn, *Int'l J. Wildland Fire* 21 (2012) 961–968.
- [19] Japanese Society of Mechanical Engineers, JSME Mechanical Engineers' Handbook, Alpha2, 2004. Maruzen (in Japanese).
- [20] K. McGrattan, S. Hostikka, R. McDermott, J. Floyd, C. Weinschenk, K. Overholt, Fire dynamics simulator, technical reference guide, in: sixth ed. Mathematical Model; Vol. 2: Verification Guide; Vol. 3: Validation Guide; Vol. 4: Configuration Management Plan, National Institute of Standards and Technology, and VTT Technical Research Centre of Finland, vol. 1, 2013.
- [21] F. Albini, Transport of firebrands by line thermals, *Combust. Sci. Technol.* 32 (1983) 277–288.
- [22] A. Muraszew, J.F. Fedele, Statistical Model for Spot Fire Spread, the Aerospace Corporation Report No. ATR-77758801, 1976. Los Angeles, CA.
- [23] C.S. Tarifa, P.P. del Notario, F.G. Moreno, On the flight paths and lifetimes of burning particles of wood, *Proc. Combust. Inst.* 10 (1965) 1021–1037.
- [24] R. Anthenian, S.D. Tse, A.C. Fernandez-Pello, On the trajectories of embers initially elevated or lofted by small scale ground fire plumes in high winds, *Fire Saf. J.* 41 (2006) 349–363.
- [25] J.P. Woycheese, Brand Lofting and Propagation for Large-scale Fires, Ph.D. Thesis, University of California, Berkeley, 2000.
- [26] K. Himoto, T. Tanaka, Transport of disk-shaped firebrands in a turbulent boundary layer, *Fire Saf. Sci.* 8 (2005) 433–444.
- [27] I.K. Knight, The design and construction of a vertical wind tunnel for the study of untethered firebrands in flight, *Fire Technol.* 37 (2007) 87–100.
- [28] H.H. Wang, Analysis of downwind distribution of firebrands sourced from a wildland fire, *Fire Technol.* 47 (2011) 321–340.
- [29] E. Koo, P.J. Pagni, D.R. Weise, J.P. Woycheese, Spotting Ignitions, In large scale fires, *Int'l J. Wildland Fire* 19 (2010) 818–843.
- [30] S. Kortas, et al., Experimental validation of a numerical model for the transport of firebrands, *Fire Saf. J.* 44 (2009) 1095–1102.
- [31] S. Suzuki, S.L. Manzello, Experiments to provide the scientific-basis for laboratory standard test methods for firebrand exposure, *Fire Saf. J.* 91 (2017) 784–790.
- [32] J.L. Pellegrino, N.P. Bryner, E.L. Johnsson, Wildland-urban Interface (WUI) fire research needs - workshop summary report, NIST Sp. 1150 (2013).